

# $\beta$ Klotho is required for metabolic activity of fibroblast growth factor 21

Yasushi Ogawa\*, Hiroshi Kurosu\*, Masaya Yamamoto\*, Animesh Nandi\*, Kevin P. Rosenblatt\*, Regina Goetz†, Anna V. Eliseenkova†, Moosa Mohammadi†, and Makoto Kuro-o\*\*

\*Department of Pathology, University of Texas Southwestern Medical Center, 6000 Harry Hines Boulevard, Dallas, TX 75390; and †Department of Pharmacology, New York University School of Medicine, 550 First Avenue, MSB 425, New York, NY 10016

Edited by Michael S. Brown, University of Texas Southwestern Medical Center, Dallas, TX, and approved March 26, 2007 (received for review February 21, 2007)

**Fibroblast growth factor 21 (FGF21) is a liver-derived endocrine factor that stimulates glucose uptake in adipocytes. Here, we show that FGF21 activity depends on  $\beta$ Klotho, a single-pass transmembrane protein whose expression is induced during differentiation from preadipocytes to adipocytes.  $\beta$ Klotho physically interacts with FGF receptors 1c and 4, thereby increasing the ability of these FGF receptors to bind FGF21 and activate the MAP kinase cascade. Knockdown of  $\beta$ Klotho expression by siRNA in adipocytes diminishes glucose uptake induced by FGF21. Importantly, administration of FGF21 into mice induces MAP kinase phosphorylation in white adipose tissue and not in tissues without  $\beta$ Klotho expression. Thus,  $\beta$ Klotho functions as a cofactor essential for FGF21 activity.**

Klotho | glucose | adipocyte | siRNA | GLUT1

Fibroblast growth factor 21 (FGF21) was identified based on cDNA sequence homology to other FGFs (1). Phylogenetic and structural analyses have assigned FGF21 to the FGF19 subfamily, which consists of FGF15 (the mouse ortholog of human FGF19), FGF19, FGF21, and FGF23 (2). The FGF19 subfamily members distinguish themselves from the other 15 FGFs in that they function in an endocrine fashion. FGF23 is secreted primarily from bone and acts on the kidney to inhibit phosphate reabsorption and vitamin D biosynthesis (3–5). FGF15 is expressed by intestinal epithelium and is involved in the negative feedback regulation of bile acid synthesis in the liver (6). FGF21 is expressed predominantly in the liver and has emerged as a metabolic regulator of glucose uptake in adipocytes during a search for novel agents with therapeutic potential to treat diabetes mellitus (7). Indeed, administration of recombinant FGF21 lowered blood glucose levels in both obese mice and in diabetic mice. Furthermore, transgenic mice that overexpress FGF21 were hypoglycemic, sensitive to insulin, and resistant to diet-induced obesity (7).

FGF21 can activate FGF receptors (FGFRs) and signaling molecules downstream, including FGFR substrate 2 $\alpha$  (FRS2 $\alpha$ ) and 44/42 MAP kinase (ERK1/2), in adipocytes (7–10). However, efforts to demonstrate a direct interaction between FGFRs and FGF21 have failed. In addition, various cell types of nonadipocyte origin including 3T3-L1 preadipocytes do not respond to FGF21 even though they express multiple FGFR isoforms (7). Furthermore, BaF3 cells that overexpress FGFRs require suprapharmacological doses of FGF21 (200–800 nM) to produce a detectable mitogenic response (8–10). These observations suggest that a cofactor(s) may be necessary for FGF21 to activate FGF signaling in adipocytes.

We and others identified Klotho, a single-pass transmembrane protein, as an essential cofactor for FGF23 to activate FGF23 signaling (11, 12). Klotho was originally identified as a gene mutated in the *klotho* mouse that exhibited phenotypes resembling human premature-aging syndromes (13). Major phenotypic overlaps were observed between Klotho-deficient mice and *Fgf23* knockout mice (14, 15), suggesting that Klotho and FGF23

may work in a common signal transduction pathway(s). Indeed, Klotho bound to multiple FGFRs and was necessary for FGF23 to bind FGFRs and activate FGF signaling in various types of cultured cells (11). In this work we show that  $\beta$ Klotho, a Klotho family protein, functions as the cofactor required for FGF21 signaling.

## Results and Discussion

**FGF21 Requires  $\beta$ Klotho to Activate FGF Signaling.** Neither FGF21 nor FGF23 signaled in parental 293 cells as evidenced by lack of induction of phosphorylation of FRS2 $\alpha$  and ERK1/2 (Fig. 1). We previously reported that ectopic overexpression of Klotho conferred responsiveness to FGF23 on 293 cells (11). However, these Klotho-overexpressing cells did not respond to FGF21. In contrast, 293 cells expressing the related  $\beta$ Klotho protein acquired the ability to respond to FGF21 (Fig. 1). We have shown that Klotho promotes FGF23 signaling by forming a ternary complex with FGF23 and FGFRs. Hence, we tested whether  $\beta$ Klotho plays a similar role in FGF21 signaling and forms a ternary complex with FGFRs.

**$\beta$ Klotho Binds to Multiple FGFRs.** The mammalian FGFRs are encoded by four distinct genes (FGFR1–FGFR4). The ectodomain of prototypical FGFRs consists of three Ig-like domains (D1–D3). A major alternative mRNA splicing event within the D3 of FGFR1–3 generates “b” and “c” isoforms, which have distinct FGF-binding specificities. An additional splicing event generates shorter FGFR1–3 isoforms lacking D1 and/or D1–D2 linker (9). We transiently expressed different FGFR isoforms, depicted in Fig. 2, and  $\beta$ Klotho in 293 cells and performed coimmunoprecipitation experiments. As shown in Fig. 2, FGFR1c and FGFR4 precipitated  $\beta$ Klotho more efficiently than the other FGFRs. In contrast, the FGFR b isoforms did not pull down  $\beta$ Klotho under these experimental conditions. The preferential binding of  $\beta$ Klotho to FGFR c isoforms and FGFR4 is reminiscent of that of Klotho (11).

Consistent with the strong interaction between  $\beta$ Klotho and FGFR1c and 4,  $\beta$ Klotho–FGFR1c and  $\beta$ Klotho–FGFR4 complexes were able to pull down FGF21 more efficiently than FGFRs alone and the other  $\beta$ Klotho–FGFR combinations,

Author contributions: Y.O. and H.K. contributed equally to this work; Y.O., H.K., and M.K. designed research; Y.O., H.K., M.Y., A.N., and M.K. performed research; A.N., K.P.R., R.G., A.V.E., and M.M. contributed new reagents/analytic tools; Y.O., H.K., and M.K. analyzed data; and Y.O., H.K., M.M. and M.K. wrote the paper.

The authors declare no conflict of interest.

This article is a PNAS Direct Submission.

Freely available online through the PNAS open access option.

Abbreviations: FGFR, fibroblast growth factor receptor; FRS, fibroblast growth factor receptor substrate; GLUT, glucose transporter; WAT, white adipose tissue.

†To whom correspondence should be addressed. E-mail: makoto.kuro-o@utsouthwestern.edu.

© 2007 by The National Academy of Sciences of the USA

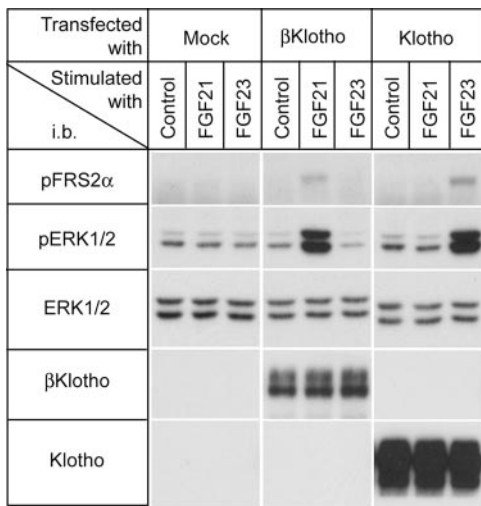


**Fig. 1.**  $\beta$ Klotho is required for FGF21 signaling. The 293 cells were transfected either with mock vector (Mock) or expression vectors for  $\beta$ Klotho and Klotho, respectively, and then stimulated with vehicle (Control) or 300 ng/ml recombinant human FGF21 or 300 ng/ml FGF23 for 10 min. Cell lysates were processed for immunoblotting with antibodies against phosphorylated FRS2 $\alpha$  (pFRS2 $\alpha$ ), phosphorylated ERK1/2 (pERK1/2), total ERK1/2 (ERK1/2),  $\beta$ Klotho, or Klotho.

demonstrating that FGF21 requires  $\beta$ Klotho to bind to its cognate FGFRs stably (Fig. 3).

**FGF21 Activity Depends on  $\beta$ Klotho Expression in Adipocytes.** Because FGF21 stimulates glucose uptake in differentiated adipocytes

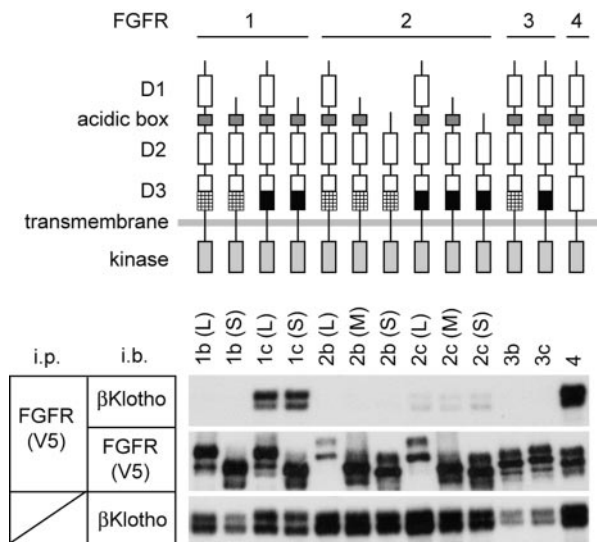


**Fig. 2.**  $\beta$ Klotho binds to multiple FGFRs. Lysates of 293 cells transfected with expression vectors for  $\beta$ Klotho and V5 epitope-tagged FGFR isoforms were incubated with anti-V5 antibody, and immunoprecipitated proteins were analyzed for the presence of  $\beta$ Klotho (Top) or FGFR (Middle). Antibodies used for immunoprecipitation (i.p.) and immunoblotting (i.b.) are indicated. Schemes for FGFR isoforms used in this work are shown above the results. The difference between b and c isoforms in FGFR1–3 resides in the C-terminal half of the third Ig-like domain (D3) are indicated in the scheme by hatched and black boxes, respectively. Another alternative splicing event occurs within the first Ig-like domain (D1) and acidic box, which generates long (L), middle (M), and short isoforms (S) in FGFR1 and FGFR2. A portion of each cell lysate sample was processed for immunoblotting with anti- $\beta$ Klotho antibody to confirm even expression of  $\beta$ Klotho among the cell samples (Bottom).

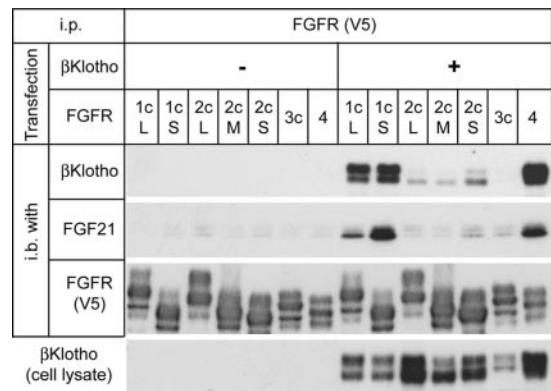


**Fig. 3.** FGF21 preferentially binds to the  $\beta$ Klotho–FGFR complex. The 293 cells transfected with FGFR alone or cotransfected with FGFR and  $\beta$ Klotho were lysed, and FGFR or the  $\beta$ Klotho–FGFR complex was pulled down from cell lysate on agarose beads carrying anti-V5 antibody. The beads were then incubated with conditioned medium containing murine FGF21, and bead-bound proteins were analyzed by immunoblotting for the presence of  $\beta$ Klotho, FGF21, and FGFR. A portion of each cell lysate sample was processed for immunoblot analysis with anti- $\beta$ Klotho antibody to confirm even expression of  $\beta$ Klotho among the cell samples (Bottom).

but not in preadipocytes (7), we reasoned that differentiated adipocytes and not preadipocytes express  $\beta$ Klotho. Indeed, we could not detect expression of  $\beta$ Klotho in preadipocytes, and furthermore, FGF21 failed to elicit a signal in these cells. The differentiated adipocytes, however, expressed  $\beta$ Klotho abundantly and responded robustly to FGF21 (Fig. 4A). To substantiate further the dependence of FGF21 on  $\beta$ Klotho, we followed  $\beta$ Klotho expression as preadipocytes differentiated into adipocytes. Expression of  $\beta$ Klotho was detected as early as day 4 and continued to increase up to day 10. This temporal increase in  $\beta$ Klotho expression correlated with the ability of FGF21 to induce phosphorylation of FRS2 $\alpha$  and ERK1/2 (Fig. 4B). We also studied time course and dose response of FGF21-induced phosphorylation of FRS2 $\alpha$  and ERK1/2. As shown in Fig. 4C, phosphorylation of FRS2 $\alpha$  and ERK1/2 became evident at 3 and 5 min, respectively, and began to decline at  $\approx$ 60 min after cell stimulation. Activation of FGF signaling was detectable with as low as 10 ng/ml (0.3 nM) FGF21 and saturated at 1,000 ng/ml (30 nM) FGF21. Lastly, we showed that endogenous  $\beta$ Klotho was able to pull down endogenous FGFR1c in differentiated adipocytes (Fig. 4D), indicating that  $\beta$ Klotho and FGFR1c form a complex under physiological conditions.

To provide more compelling evidence for the dependence of FGF21 signaling on  $\beta$ Klotho, we knocked down  $\beta$ Klotho expression in differentiated adipocytes by using an siRNA approach. Four independent siRNAs against different sequences in  $\beta$ Klotho suppressed activation of both FRS2 $\alpha$  and ERK1/2 by FGF21 (Fig. 5A) and more importantly, abolished the effect of FGF21 on glucose uptake, indicating that  $\beta$ Klotho is essential for FGF21 to exert its metabolic activity on adipocytes (Fig. 5B).

FGF21-induced glucose uptake in adipocytes is accompanied by up-regulation of glucose transporter 1 (GLUT1), which is known to regulate insulin-independent glucose uptake, but not glucose transporter 4 (GLUT4), which primarily contributes to insulin-dependent glucose uptake (7, 16). Therefore, we determined GLUT1 and GLUT4 protein levels and found that the knockdown of  $\beta$ Klotho expression by siRNA also attenuated the ability of FGF21 to increase GLUT1 expression (Fig. 5C). Thus, FGF21– $\beta$ Klotho signaling may be an important regulator in insulin-independent glucose uptake in adipocytes.

Insulin produced a greater increase in glucose uptake than

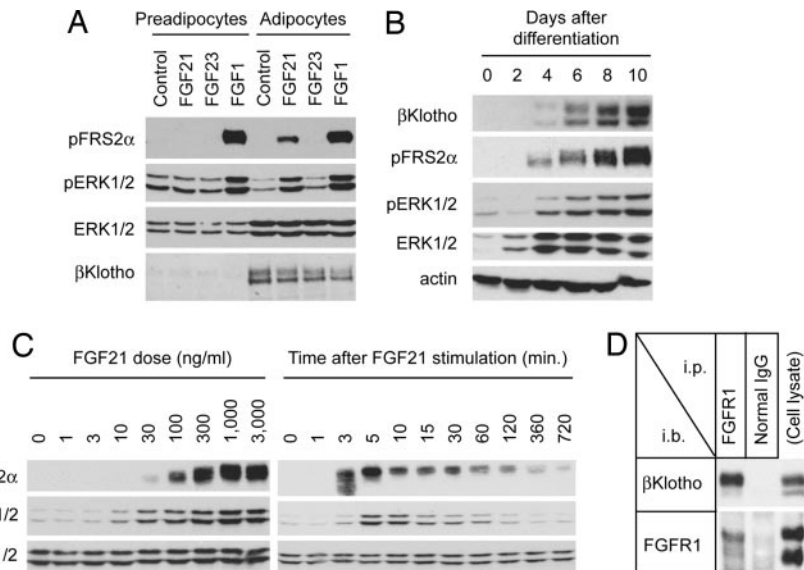


**Fig. 4.** Adipocytes expressing  $\beta$ Klotho respond to FGF21. (A) FGF21 activates FRS2 $\alpha$  and ERK1/2 in differentiated 3T3-L1 adipocytes. 3T3-L1 preadipocytes and differentiated adipocytes were stimulated with conditioned medium containing murine FGF21 or murine FGF23. The same volume of conditioned medium from mock-transfected 293 cells was used as a negative control (Control). Recombinant FGF1 (100 ng/ml) was used as a positive control. (B)  $\beta$ Klotho is expressed upon differentiation of preadipocytes to adipocytes. Differentiation of 3T3-L1 preadipocytes was induced, and the cells were stimulated for 10 min with the FGF21-containing conditioned medium on the indicated days after differentiation. Cell lysate was prepared for immunoblot analysis with the antibodies indicated. (C) Dose response and time course of FGF21 signaling in 3T3-L1 adipocytes. Differentiated 3T3-L1 adipocytes were stimulated with increasing doses of recombinant human FGF21 for 10 min (Left) or stimulated with 1  $\mu$ g/ml recombinant human FGF21 for various time periods (Right). Cell lysates were subjected to immunoblot analysis by using the antibodies indicated. (D) Endogenous  $\beta$ Klotho and FGFR1c form a complex in adipocytes. Lysate of 3T3-L1 adipocytes was subjected to immunoprecipitation (i.p.) with anti-FGFR1 antibody or normal IgG followed by immunoblot (i.b.) analysis with anti- $\beta$ Klotho antibody or anti-FGFR1 antibody. Cell lysate prepared from differentiated 3T3-L1 adipocytes (Upper, representing 5% of the input) or from 293 cells transfected with FGFR1c(L) and FGFR1c(S) (Lower, serving as size markers for these receptors) was directly subjected to immunoblot analysis to verify the presence of  $\beta$ Klotho and FGFR1c, respectively (Cell lysate).

FGF21 in 3T3-L1 adipocytes (data not shown). However, this finding may not necessarily mean that the impact of FGF21 on glucose metabolism is insignificant. The effect of FGF21 on glucose uptake becomes evident several hours after the stimulation and lasts for 24 h or longer (7) even though FGF21-induced Akt phosphorylation diminishes within 30 min in 3T3-L1 adipocytes (17). In contrast, insulin-induced glucose uptake becomes evident within minutes after stimulation in these cells and attenuates within hours. The prolonged effect of FGF21 may influence glucose metabolism under physiological settings. In fact, FGF21 has a potent and sustained blood glucose-lowering effect when administered into diabetic and obese mice (7). These observations imply that FGF21 and insulin play distinct roles in the regulation of glucose metabolism: FGF21 induces a moderate and sustained increase in glucose uptake primarily through up-regulating GLUT1 expression, whereas insulin induces a strong and transient increase through promoting GLUT4 translocation from the intracellular pool to the plasma membrane.

To determine the dependence of FGF21 signaling on  $\beta$ Klotho in an *in vivo* setting, we injected FGF21 into mice and analyzed ERK1/2 phosphorylation in white adipose tissue (WAT), skeletal muscle, and kidney. Importantly,  $\beta$ Klotho was expressed in WAT but not in the skeletal muscle or kidney (Fig. 6A). Consistent with the expression pattern of  $\beta$ Klotho, FGF21 induced ERK1/2 phosphorylation only in WAT (Fig. 6B). As a control, injection of FGF23 into mice stimulated ERK1/2 phosphorylation only in the kidney where Klotho is expressed (Fig. 6C). These data provide strong *in vivo* evidence for requirement of  $\beta$ Klotho and Klotho in FGF21- and FGF23-mediated tissue response, respectively.

**The Klotho Gene Family Regulates Metabolic Activities of FGF Hormones.** In this work, we show that  $\beta$ Klotho is expressed in adipocytes and enables FGF21 to bind to and activate its cognate

FGFRs, leading to increased glucose uptake. This dependence of FGF21 on  $\beta$ Klotho represents the mechanism by which FGF21 acts specifically on adipose tissue. Similarly, we and others have demonstrated that Klotho enables FGF23 to bind and activate its cognate FGFRs.  $\beta$ Klotho was isolated based on cDNA sequence homology to Klotho (18). The  *$\beta$ klotho* gene encodes a single-pass transmembrane protein that shares 41% amino acid identity with Klotho and in addition to adipose tissue is also expressed in liver and pancreas. Mice deficient in  $\beta$ Klotho have overlapping phenotypes with mice lacking FGF15 or FGFR4 (6, 19, 20). These phenotypes include increased bile acid synthesis and increased expression of two key bile acid synthases, CYP7A1 and CYP8B1, in the liver. Based on these genetic data and studies with primary hepatocytes, a model has emerged in which FGF15/FGF19 and FGFR4 and  $\beta$ Klotho cooperate to regulate bile acid synthesis negatively (6). Thus, it seems plausible that  $\beta$ Klotho acts also as a cofactor in FGF19/15 signaling.

In summary, the Klotho gene family may have evolved to confer tissue-specific bioactivity on FGF19 subfamily members. Further investigations on Klotho and  $\beta$ Klotho are expected to provide more insight into the molecular mechanisms by which the FGF19 subfamily regulates glucose metabolism, bile acid synthesis, and phosphate/vitamin D metabolism. FGF21 and FGF23 may play a pathogenetic role in human diseases such as diabetes, obesity, chronic kidney disease, and bone disorders. Klotho and  $\beta$ Klotho will be important targets of research when exploring therapeutic application of these endocrine FGFs.

## Materials and Methods

**Expression Vectors.** Expression vectors for mouse FGFRs with a V5 epitope tag at the C terminus and murine FGF23 (R179Q) were described previously (11). The murine  $\beta$ Klotho cDNA was obtained by reverse transcriptase PCR from mRNAs of differ-

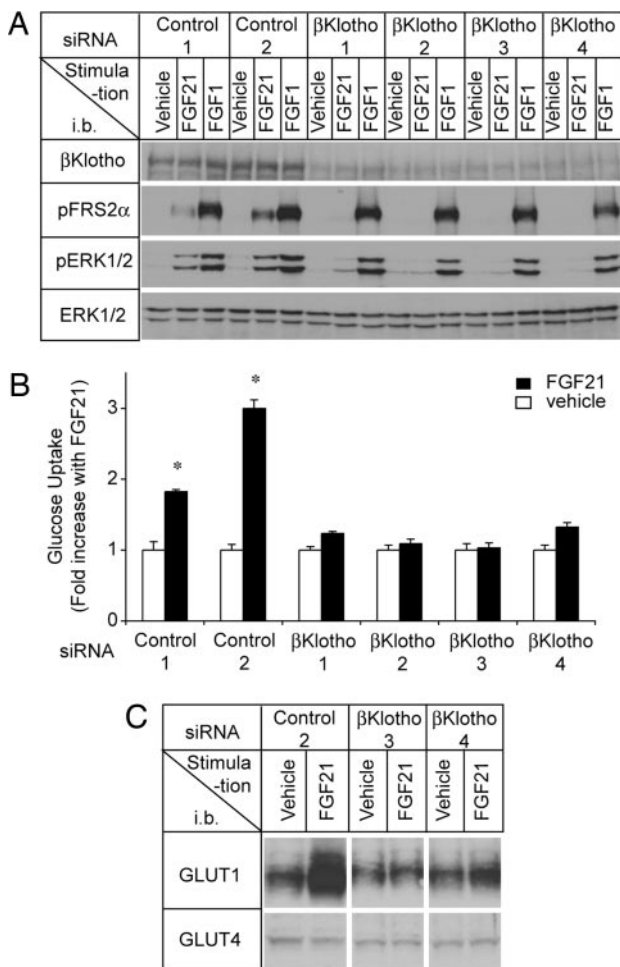


**Fig. 5.** FGF21 requires  $\beta$ Klotho to activate FGF signaling, increase glucose uptake, and increase GLUT1 expression in adipocytes. (A) Differentiated 3T3-L1 adipocytes were transfected with four different siRNAs for  $\beta$ Klotho ( $\beta$ Klotho 1–4) or nontargeting control siRNAs (Control 1, 2); 2 days after transfection, the cells were stimulated for 10 min with recombinant human FGF21, FGF1, or vehicle. Cell lysates were immunoblotted (i.b.) with antibodies as indicated. (B) Differentiated 3T3-L1 adipocytes transfected with  $\beta$ Klotho or control siRNAs as in A were incubated for 18 h either with recombinant human FGF21 or with vehicle and then assayed for glucose uptake. The results are presented as means  $\pm$  SD error bars ( $n = 3$ ). \*,  $P < 0.001$  by Student's *t* test. (C) Expression of GLUT1 and GLUT4 was determined by immunoblot analysis by using the cell lysates from B.

entiated 3T3-L1 adipocytes. cDNA encoding murine FGF21 (IMAGE Clone; Invitrogen, Carlsbad, CA) or murine  $\beta$ Klotho was cloned into pEF1 expression vector (Invitrogen). Before subcloning, a FLAG epitope tag was added to the C terminus of  $\beta$ Klotho, and appropriate restriction enzyme sites were added to both ends by using synthetic oligonucleotides and PCR.

**Cell Culture.** The 3T3-L1 preadipocytes (American Type Culture Collection, Rockville, MD) were maintained in DMEM containing 10% calf serum (Mediatech, Herndon, VA). Differentiation to adipocytes was induced by culturing the cells for 2 days in differentiation medium [DMEM (American Type Culture Collection)/10% FBS/10 mM HEPES/MEM nonessential amino acids (NEAA)/penicillin/streptomycin (PC/SM) (all from Invitrogen)/2  $\mu$ M insulin/1  $\mu$ M dexamethasone/0.25 mM 3-isobutyl-1-methylxanthine (IBMX) (all from Sigma-Aldrich, St. Louis, MO)] and then culturing in differentiation medium without dexamethasone and IBMX for another 2 days. There-

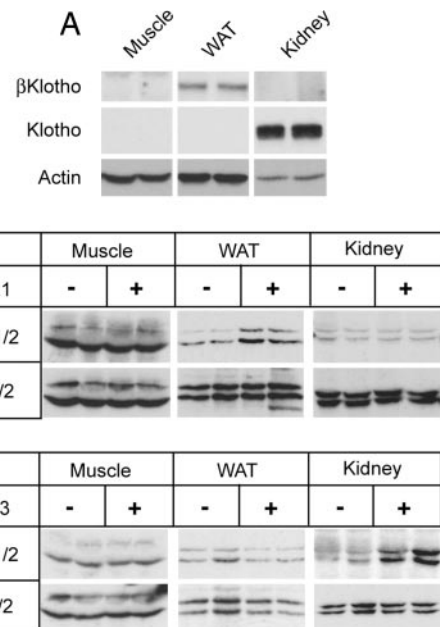


**Fig. 6.** FGF21 activates FGF signaling in WAT in mice. (A) Expression of  $\beta$ Klotho and Klotho in hindlimb muscle (Muscle), perigonadal fat pad tissue (WAT), and kidney from two wild-type mice was examined by immunoblot analysis. Actin blot is shown as a loading control. (B) Muscle, fat, and renal tissues were excised from mice treated either with recombinant human FGF21 ( $n = 2$ ) or with vehicle ( $n = 2$ ). Tissue lysates were prepared for immunoblot analysis by using the antibodies indicated. (C) As in B, except that recombinant human FGF23 was injected into mice.

after, the medium was changed every 2 days with DMEM supplemented with 10% FBS/10 mM HEPES/NEAA/PC/SM. Accumulation of lipid droplets was observed in >95% of cells after 7 days, and the cells at day 7–10 were used for experiments.

**Preparation of FGF21 and FGF23.** Human recombinant FGF21 and FGF23 (R179Q) were expressed in *Escherichia coli*, refolded *in vitro*, and purified by affinity, ion-exchange, and size-exclusion chromatographies following a previously published protocol (21). Serum-free conditioned medium containing murine FGF21 was collected from 293 cells transiently transfected with the FGF21 expression vector. The activity of FGF21 in the cell culture medium was determined by comparing its ability to induce ERK1/2 phosphorylation in differentiated 3T3-L1 adipocytes with that of recombinant human FGF21 of known concentration. The activity of murine FGF23 (R179Q) present in the cell culture medium was determined by using 293 cells stably expressing Klotho as described previously (11). Conditioned medium with activity equivalent to that of 2,000 ng/ml (67 nM) recombinant human FGF21 and 300 ng/ml (10 nM) FGF23, respectively, was used to stimulate cultured cells. The same amount of serum-free conditioned medium from mock-transfected 293 cells was used as a negative control.

**Immunoprecipitation and Immunoblotting.** Subconfluent 293 cells were transfected with expression vectors for  $\beta$ Klotho and FGFRs 36 h before the experiments by using Lipofectamine as carrier (Invitrogen). The cells were lysed in buffer containing inhibitors for phosphatase and proteinase as described previously (22). After saving a portion of each cell lysate sample for immunoblotting with anti- $\beta$ Klotho antibody, the cell lysates were incubated with anti-V5-agarose beads (Sigma-Aldrich) at 4°C for 3 h. The beads were washed four times with Tris-buffered saline containing 1% Triton X-100 (TBST); bead-bound proteins were eluted with Laemmli

sample buffer, electrophoresed, and then transferred to Hybond C Extra membrane (Amersham Biosciences, Piscataway, NJ). The protein blots were incubated with anti- $\beta$ Klotho antibody (R&D Systems, Minneapolis, MN) or anti-V5 antibody (Invitrogen) followed by horseradish peroxidase-conjugated anti-goat IgG (Santa Cruz Biotechnology, Santa Cruz, CA) or anti-mouse IgG (Amersham Biosciences). Chemiluminescence signals were developed with the SuperSignal West Dura system (Pierce, Rockford, IL). For detection of endogenous interaction between  $\beta$ Klotho and FGFR1c in differentiated 3T3-L1 adipocytes, cell lysate samples were incubated with anti-FGFR1c antibody (Santa Cruz Biotechnology) and protein G-Sepharose at 4°C for 2 h. The Sepharose beads were washed four times with complete lysis buffer and then twice with lysis buffer lacking Triton X-100. Bead-bound proteins were eluted with Laemmli sample buffer and subjected to immunoblot analysis by using anti- $\beta$ Klotho or anti-FGFR1c antibody.

**FGF21 Pull-Down Experiments.** Cell lysate samples prepared from 293 cells transfected with FGFR alone or from 293 cells co-transfected with FGFR and  $\beta$ Klotho were incubated with anti-V5-agarose beads at 4°C for 3 h. The beads were washed four times with TBST and then incubated with serum-free conditioned medium containing murine FGF21 at 4°C for 3 h. Thereafter, the beads were washed three times with Krebs-Ringer-Hepes buffer (118 mM NaCl/4.96 mM KCl/2.54 mM CaCl<sub>2</sub>/1.19 mM KH<sub>2</sub>PO<sub>4</sub>/1.19 mM MgSO<sub>4</sub>/20 mM Hepes, pH 7.4) containing 1% Triton X-100 followed by three washes with the same buffer lacking Triton X-100. Bead-bound proteins were eluted with Laemmli sample buffer and subjected to immunoblot analysis by using anti-V5 antibody, anti- $\beta$ Klotho antibody, or anti-mouse FGF21 antibody (R&D Systems).

**Immunoblot Analysis of FGF Signaling.** Cells cultured on multiwell plates were serum-starved overnight and then treated for 10 min either with human recombinant FGF21 or FGF23 (R179Q) or FGF1 (FGF1 was from Upstate Biotechnology, Lake Placid, NY). The cells were snap-frozen in liquid nitrogen and processed for immunoblot analysis by using anti-phospho-FRS2 $\alpha$  antibody (Cell Signaling Technology, Beverly, MA), anti-phospho-44/42 MAP kinase (ERK1/2) antibody (Cell Signaling Technology), and anti-ERK antibody (Cell Signaling Technology) as described previously. Wild-type, 8-week-old, male inbred 129sv mice were administered either human recombinant FGF21 (0.3  $\mu$ g g<sup>-1</sup> body weight) or FGF23 (R179Q, 0.1  $\mu$ g g<sup>-1</sup> body weight) or vehicle (10 mM Hepes, pH 7.4/150 mM NaCl) by injection into the inferior vena cava. Perigonadal fat pads, kidneys, and hind limb muscles were excised 15, 17, and 19 min, respectively, after protein injection. The tissues were flash-frozen in liquid nitrogen and processed for immunoblot analysis by using anti-phospho-ERK, anti-ERK, and anti-actin (Chemicon International, Temecula, CA) antibodies. All animal experiments were approved by the Institutional Animal Care and Research Advisory Committee of the University of Texas Southwestern Medical Center at Dallas.

**Knockdown of  $\beta$ Klotho by RNA Interference.** 3T3-L1 adipocytes were transfected with siRNA duplexes by electroporation as described previously (23). Briefly, differentiated 3T3-L1 adipo-

cytes were harvested by using 0.5 mg/ml collagenase (Sigma-Aldrich), washed twice with PBS, and suspended in PBS (2  $\times$  10<sup>7</sup> per ml). The cells were mixed with 5 nmol per 10<sup>7</sup> cells of siRNA oligonucleotide against four different sequences in  $\beta$ Klotho ( $\beta$ Klotho 1: sense, CGU GUU UGG UUA UAC GGC CUG GAC U; antisense, AGU CCA GGC CGU AUA ACC AAA CAC G;  $\beta$ Klotho 2: sense, CGC AGU UUA CCG AUC CUC ACC UGU A; antisense, UAC AGG UGA GGA UCG GUA AAC UGC G;  $\beta$ Klotho 3: sense, CAG UUU GCU CUG GAC UGG ACC UCU A; antisense, UAG AGG UCC AGU CCA GAG CAA ACU G;  $\beta$ Klotho 4: sense, GCG GAA GAC ACA GAC UGC ACC AUU U; antisense, AAA UGG UGC AGU CUG UGU CUU CCG C; Invitrogen) or nontargeting randomized sequences (control 1: sense, CAG UCG UGG UCG UCA CCA GUU UCU A; antisense, UAG AAA CUG GUG ACG ACC ACG ACU G; control 2: sense, GCG CAG AGA CAG UCA CCA CAA GUU U; antisense, AAA CUU GUG GUG ACU GUC UCU GCG C; Invitrogen), and electroporated with a gene pulser system at the setting of 0.18 kV and 960  $\mu$ F capacitance (Bio-Rad, Hercules, CA). Immediately after electroporation, the cells were mixed with complete medium and incubated for 10 min before reseeding onto collagen I-coated 12-well plates (Becton Dickinson Labware, Bedford, MA). Thirty to forty hours after transfection, the cells were serum-starved overnight and then stimulated with FGF21 or FGF1 and assayed for phosphorylation of FRS2 $\alpha$  and ERK1/2 and for glucose uptake

**Glucose Uptake Assay.** Differentiated 3T3-L1 cells transfected with either  $\beta$ Klotho siRNA or control siRNA were treated with 1  $\mu$ g/ml human recombinant FGF21 in DMEM supplemented with 0.1% free fatty acid (FFA)-free BSA (Sigma-Aldrich) for 18 h at 37°C. Unstimulated cells served as a negative control. The wells were washed with Krebs-Ringer-Hepes buffer supplemented with 0.1% FFA-free BSA and then incubated in the same buffer supplemented with 2-deoxy-D-[1-<sup>3</sup>H]glucose (0.4  $\mu$ Ci, 0.1 mM; Amersham Biosciences) for 1 h. The reaction was stopped by washing the cells twice with ice-cold PBS containing 20  $\mu$ M cytochalasin B (Sigma-Aldrich) followed by snap-freezing in liquid nitrogen. Cell-associated radioactivity was determined by liquid scintillation counting. Nonspecific deoxyglucose uptake was measured in the presence of 50  $\mu$ M cytochalasin B and subtracted from each sample to obtain specific uptake. A portion of each cell sample was saved immediately before the addition of D-[2-<sup>3</sup>H]glucose and processed for immunoblotting with anti- $\beta$ Klotho antibody, anti-GLUT1 antibody (H-43; Santa Cruz Biotechnology) and anti-GLUT4 antibody (H-61; Santa Cruz Biotechnology).

We thank E. C. Friedberg at the University of Texas (UT) Southwestern for critical reading of the manuscript and T. Inagaki, M. Choi, and S. Kliewer at UT Southwestern for helpful discussion. This work was supported in part by grants from The Eisai Research Fund (to M.K.), Ellison Medical Foundation Grant AG-SS-1459-05 (to M.K.), The Ted Nash Long Life Foundation (to M.K.), the Irma T. Hirsch Fund (to M.M.), and National Institutes of Health Grants R01AG19712 (to M.K.), R01AG25326 (to M.K. and K.P.R.), and R01DE13686 (to M.M.).

- Nishimura T, Nakatake Y, Konishi M, Itoh N (2000) *Biochim Biophys Acta* 1492:203–206.
- Itoh N, Ornitz DM (2004) *Trends Genet* 20:563–569.
- The ADHR Consortium (2000) *Nat Genet* 26:345–348.
- Quarles LD (2003) *Am J Physiol* 285:E1–E9.
- Schiavi SC, Kumar R (2004) *Kidney Int* 65:1–14.
- Inagaki T, Choi M, Moschetta A, Peng L, Cummins CL, McDonald JG, Luo G, Jones SA, Goodwin B, Richardson JA, et al. (2005) *Cell Metab* 2:217–225.
- Kharitonov A, Shiyanova TL, Koester A, Ford AM, Micanovic R, Galbreath EJ, Sandusky GE, Hammond LJ, Moyers JS, Owens RA, et al. (2005) *J Clin Invest* 115:1627–1635.
- Ibrahimi OA, Zhang F, Eliseenkova AV, Itoh N, Linhardt RJ, Mohammadi M (2004) *Hum Mol Genet* 13:2313–2324.
- Mohammadi M, Olsen SK, Ibrahimi OA (2005) *Cytokine Growth Factor Rev* 16:107–137.
- Zhang X, Ibrahimi OA, Olsen SK, Umemori H, Mohammadi M, Ornitz DM (2006) *J Biol Chem* 281:15694–15700.
- Kurosu H, Ogawa Y, Miyoshi M, Yamamoto M, Nandi A, Rosenblatt KP, Baum MG, Schiavi S, Hu MC, Moe OW, Kuro-o M (2006) *J Biol Chem* 281:6120–6123.
- Urakawa I, Yamazaki Y, Shimada T, Iijima K, Hasegawa H, Okawa K, Fujita T, Fukumoto S, Yamashita T (2006) *Nature* 444:770–774.

13. Kuro-o M, Matsumura Y, Aizawa H, Kawaguchi H, Suga T, Utsugi T, Ohyama Y, Kurabayashi M, Kaname T, Kume E, *et al.* (1997) *Nature* 390:45–51.
14. Shimada T, Kakitani M, Yamazaki Y, Hasegawa H, Takeuchi Y, Fujita T, Fukumoto S, Tomizuka K, Yamashita T (2004) *J Clin Invest* 113:561–568.
15. Razzaque MS, Sitara D, Taguchi T, St-Arnaud R, Lanske B (2006) *FASEB J* 20:720–722.
16. Pessin JE, Bell GI (1992) *Annu Rev Physiol* 54:911–930.
17. Moyers JS, Shyanova TL, Mehrbod F, Dunbar JD, Noblitt TW, Otto KA, Reifel-Miller A, Kharitonov A (2007) *J Cell Physiol* 210:1–6.
18. Ito S, Kinoshita S, Shiraishi N, Nakagawa S, Sekine S, Fujimori T, Nabeshima Y (2000) *Mech Dev* 98:115–119.
19. Ito S, Fujimori T, Furuya A, Satoh J, Nabeshima Y, Nabeshima Y (2005) *J Clin Invest* 115:2202–2208.
20. Yu C, Wang F, Kan M, Jin C, Jones RB, Weinstein M, Deng CX, McKechnan WL (2000) *J Biol Chem* 275:15482–15489.
21. Plotnikov AN, Hubbard SR, Schlessinger J, Mohammadi M (2000) *Cell* 101:413–424.
22. Kurosu H, Yamamoto M, Clark JD, Pastor JV, Nandi A, Gurnani P, McGuinness OP, Chikuda H, Yamaguchi M, Kawaguchi H, *et al.* (2005) *Science* 309:1829–1833.
23. Jiang ZY, Zhou QL, Coleman KA, Chouinard M, Boese Q, Czech MP (2003) *Proc Natl Acad Sci USA* 100:7569–7574.